

## Optically plugged quadrupole trap for Bose-Einstein condensates

D. S. Naik and C. Raman\*

*School of Physics, Georgia Institute of Technology, Atlanta, Georgia 30332, USA*

(Received 9 September 2004; published 14 March 2005)

We created sodium Bose-Einstein condensates in an optically plugged quadrupole magnetic trap. A focused, 532-nm laser beam repelled atoms from the coil center where Majorana loss is significant. We produced condensates containing up to  $3 \times 10^7$  atoms, a factor of 60 improvement over previous work and a number comparable to the best all-magnetic traps, and transferred up to  $9 \times 10^6$  atoms into a purely optical trap. We compare our observations with a simple model of evaporative cooling, concluding that a laser in the range of 1 W (rather than 5 W) may suffice.

DOI: 10.1103/PhysRevA.71.033617

PACS number(s): 03.75.Mn, 03.75.Nt, 32.80.Lg, 32.80.Pj

Large-volume magnetic traps are a workhorse in the field of quantum gases [1]. This is due to the fact that they can capture an entire laser-cooled atom cloud, a feature difficult to achieve with optical traps [2–4], one which greatly facilitates achieving the initial conditions for evaporative cooling. Among such traps, the quadrupole design [see Fig. 1(a)] has the largest capture volume—close to the physical size of the coils—and tightest confinement due to the linearity of the potential. Moreover, only one pair of coils is required, and this maximizes the optical access to the atoms. While these advantages are extremely appealing, there is one crucial drawback—the magnetic field zero at the center near which atoms are eventually lost. Magnetic trap designs without a field zero at the minimum typically require additional coils that reduce the visibility of the atom cloud. The modified quadrupole trap with an “optical plug” introduced by Ketterle and co-workers solved the problem of the field zero without compromising optical access [5]. However, it was not clear to what extent it could be improved relative to other successful designs [1].

In this work, we demonstrate that an optically plugged quadrupole trap (OPT) is a simple and robust method of creating a Bose-Einstein condensate (BEC) that performs as well as the best Ioffe-Pritchard (IP) traps. Our main result is a 60-fold improvement in atom number over earlier work, achieving the third-largest alkali-metal BEC reported [6,7]. Our design uses a stable, solid state “plug” laser at 532 nm requiring little or no adjustment for several weeks of operation. Moreover, the focusing of an additional, intense laser beam adds only a minor complexity to the apparatus, comparable to that required for optical confinement of BECs [8]. We studied the effect of the plug laser power, concluding that a laser in the range of 1 W (rather than  $\sim 5$  W, as was used earlier) might suffice to create a BEC. While the OPT does not have a simple harmonic potential energy surface (see below), we have transferred up to  $9 \times 10^6$  atoms into a purely optical trap created by a single, focused infrared laser beam. This demonstrates that the OPT is an excellent starting point for BEC experiments.

A simple configuration of coils that will trap low mag-

netic field seeking particles is the quadrupole trap, formed by a pair of coils running current in the opposite direction in the so-called “anti-Helmholtz” configuration [see Fig. 1(a)]. Unfortunately, by itself this trap is not so useful for evaporative cooling—within a region of 1–2  $\mu\text{m}$  radius near the magnetic field zero at the trap center, the atoms can spontaneously undergo spin flips and are lost from the trap [9]. This Majorana loss can be eliminated if one removes the field zero from the cloud, for example, using a fast, rotating bias field [9,10], or alternately, using a Ioffe-Pritchard design which has a finite bias field at the trap minimum [11]. Our approach is based on an idea of Ketterle and co-workers to use the optical dipole force of a blue-detuned laser beam to repel atoms from the region containing the hole [5]. The resulting potential energy surface depends on both laser and magnetic fields, and the minimum is displaced from the coil center so that the atoms experience a nonzero magnetic field.

Our experimental sequence starts with a Zeeman-slowed  $^{23}\text{Na}$  atomic beam based on a “spin-flip” design whose flux is about  $10^{11}$  atoms/s. About  $10^{10}$  atoms are loaded in 3 s into a dark magneto-optical trap (MOT) in the  $F=1$  hyperfine level [12]. Roughly 1/3 of the atoms (the weak-field seekers) are transferred into the OPT (the magnet and laser beam are turned on simultaneously), whose axis of symmetry is vertical. Each coil has 24 windings of 1/8 in. square cross-section copper tubing. The average diameter of each coil is 4 in. and their spacing is 2.25 in. A current of 350 A flows through the tube walls, while cooling water flows through the tube itself, and the total voltage drop including a high current switch is 20 V. The predicted field gradient is 320 G/cm at this current. Following the loading of the trap, rf evaporative cooling for 42 s resulted in an almost pure Bose-Einstein condensate of  $(10\text{--}30) \times 10^6$  atoms. In order to achieve such high atom numbers, we reduced the trap current by a factor of 14 toward the end of the evaporation stage, thus lowering inelastic losses associated with high atomic density. To ensure the magnetic field zero did not move with respect to the stationary plug beam, it was imperative to carefully cancel stray magnetic fields. By observing the motion of the cloud center and adjusting three pairs of Helmholtz coils, we reduced stray dc fields to  $\lesssim 20$  mG, resulting in  $\lesssim 10\text{-}\mu\text{m}$  motion of the field zero, well below the plug beam diameter.

\*Electronic address: craman@gatech.edu

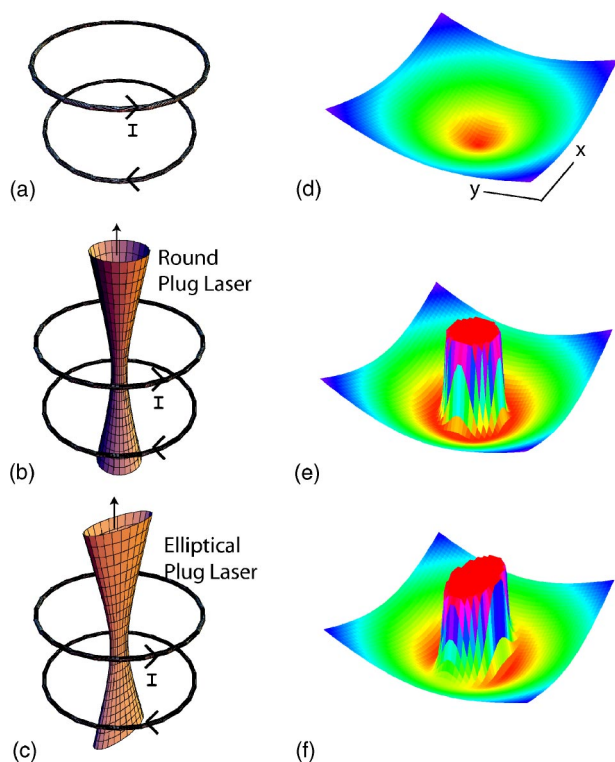


FIG. 1. The optically plugged trap (OPT). (a) A pair of coils with opposite currents constitutes a quadrupole trap, which has a hole in the center where atoms are lost by Majorana spin flips. (b) An optically plugged trap is realized by focusing an intense, blue-detuned laser beam to the center that repels atoms from the hole, resulting in a Bose-Einstein condensate free to move along a ring. (c) Using an elliptically shaped focus, the symmetry of the ring is broken, and two distinct minima form along the minor axis of the ellipse. About each minimum the atoms experience three-dimensional, harmonic confinement with three distinct frequencies. (d)–(f) Potential energy versus position in the  $x$ - $y$  plane corresponding to the trapping geometries of (a)–(c).

The plug beam is derived from a 5-W, intracavity-doubled Nd:YVO<sub>4</sub> laser (Coherent Verdi-5W) at 532 nm. The laser output passes through a 40-MHz acousto-optic modulator (AOM) (Intra-Action Corp.) used for rapid switch-off of the laser beam. After expanding the beam size by a factor of 3, we focused it into the vacuum chamber to a beam waist of  $\approx 40 \mu\text{m}$  using a 500-mm lens. The green light propagates along the axis of the quadrupole field (in our notation, the  $z$  axis) through the vacuum chamber and its focus is subsequently imaged onto a charge-coupled device camera with a magnification of 2.5. We used the same imaging path to record the atomic absorption using a resonant probe laser at 589 nm. To suppress the powerful green laser beam during this measurement, we placed a dichroic mirror, a 589-nm interference filter and up to two bandpass edge filters in the beam path, for a total suppression of up to 13 orders of magnitude. The focus of the plug beam was aligned to the center of the atom cloud in the trap by steering the beam output before the final focusing lens using a mirror mount with a micrometer actuator. After coarsely positioning the focus at the center of the circular absorption image, we per-

formed a fine-tuning by searching for an enhancement of evaporative cooling, as detailed below.

*Ring trap.* To understand the potential energy surface of the combined optical and magnetic fields, we consider an ideal case of a perfect Gaussian laser beam profile. Since the quadrupole potential possesses azimuthal symmetry [see Fig. 1(b)], this results in a ring-shaped Bose-Einstein condensate. Neglecting the variation of the laser beam along  $z$  due to the long Rayleigh range of a few millimeters, the minimum of the combined laser and magnetic potential is a circle of radius  $r_0$  in the  $x$ - $y$  plane, which is located midway between the coils [see Fig. 1(e)].  $r_0$  satisfies  $(\partial/\partial r)U_0 e^{-2r^2/W^2}|_{r=r_0} = \mu B'/2$ , with  $U_0$  the peak ac Stark shift from the plug beam,  $W$  the beam waist,  $B'$  the axial quadrupole magnetic field gradient, and  $\mu = 1/2$  Bohr magneton is the magnetic moment for atoms in the  $|F=1, m_F=-1\rangle$  hyperfine state. Typically,  $r_0 > W$ . Near  $r=r_0$  and  $z=0$ , the potential  $U$  varies harmonically in the  $r$  and  $z$  directions, with radial curvature  $\partial^2 U/\partial r^2 = \mu B'/(2r_0)(4r_0^2/W^2 - 1)$ . Along the  $z$  direction  $\partial^2 U/\partial z^2 = 2\mu B'/r_0$ .

*Harmonic trap.* Our laser profile deviates considerably from a perfect Gaussian in the wings, where the atoms primarily reside. Small imperfections can result in minima whose location and curvature about the minimum are uncontrolled. To exert control over the potential, we artificially broke the symmetry using an elliptical focus of aspect ratio  $a$ . We inserted a slit into the beam path before the final focusing lens to create a spatial profile with roughly the inverted aspect ratio  $1/a$ . The resulting beam focus was elliptical, with its minor axis orthogonal to the slit direction. The resulting potential has two distinct minima on the minor axis  $y$  of the ellipse at  $y = \pm y_0$  [see Fig. 1(c) and 1(f)]. Typically,  $W_y = 42 \mu\text{m}$  and  $W_x = aW_y$ , with  $a = 2.5$ ,  $B' = 23 \text{ G/cm}$  in our decompressed trap, and we estimate  $y_0 = 70 \mu\text{m}$  and  $U_0/k_B = 65 \mu\text{K}$  for 2.7 W of laser power delivered to the atoms.

The elliptical focus allows us to impose a hierarchy of trapping frequencies  $\omega_y > \omega_z > \omega_x$  that simplifies the time-of-flight images, as shown below. A randomly located focus would have arbitrary values for the frequencies. Neglecting gravity and assuming  $a \rightarrow \infty$ , one has  $\omega_x^2 = \mu B'/(2My_0)$ ,  $\omega_y^2 = \omega_x^2(4y_0^2/W^2 - 1)$ , and  $\omega_z^2 = 4\omega_x^2$ . For our parameters, gravity and the finite value of  $a$  introduce corrections of 10% to  $\omega_x$  and  $\omega_z$ , yielding predicted frequencies of  $\omega_{x,y,z} = 2\pi \times 60, 215, \text{ and } 125 \text{ Hz}$ , respectively. In practice, there can also be an asymmetry between the two minima which is discussed later.

The presence of an elliptical focus dramatically changed the time-of-flight distribution of the trapped gas. For final rf frequencies above 500 kHz we observed a symmetric distribution in the  $x$ - $y$  plane when imaged along the  $z$  direction, indicating a thermal cloud [Fig. 2(a)]. Below 500 kHz we observed a bimodal distribution with an anisotropically expanding condensate in the shape of a cigar [Figs. 2(b) and 2(c)]. The long axis of the cigar was parallel to the minor axis of the ellipse. While we expect that this axis should rotate if the ellipse is made to rotate, we could not easily observe this simply by rotating the slits due to a residual ellipticity in the laser beam profile. At a frequency of 150 kHz we saw a nearly pure condensate. Time-of-flight images

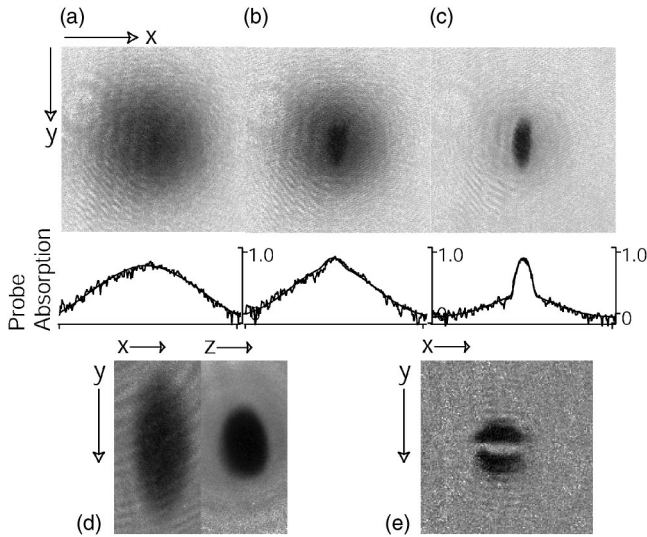


FIG. 2. Transition to BEC in the OPT. Absorption images taken at final rf frequencies of (a) 0.55, (b) 0.45, (c) 0.30 MHz show the formation of a Bose condensate. The field of view in each image is  $2.7 \times 2.7 \text{ mm}^2$ . Below each image is a horizontal slice through a two-dimensional bimodal fit to the absorption data. (d) Views along the  $z$  and  $x$  directions (40 and 20 ms time of flight, respectively) show the three-dimensional anisotropic expansion of the condensate. (e) A view in the trap along the  $z$  direction shows two separated clouds near the two minima of the potential. Each view in (d) is  $1.6 \text{ mm}$  ( $y$ )  $\times$   $0.8 \text{ mm}$  ( $x, z$ ), while (e) is  $0.8 \text{ mm} \times 0.8 \text{ mm}$ .

from the side ( $x$  direction) showed that the condensate expanded anisotropically in three dimensions [Fig. 2(d)].

The measured temperature just above the transition was  $1.9 \mu\text{K}$ . The theoretical prediction for a harmonically trapped ideal gas is  $T_c = (\hbar\bar{\omega}/k_B)(N/1.202)^{1/3}$ , where  $\bar{\omega} = (\omega_x\omega_y\omega_z)^{1/3}$  [13]. For the estimated frequencies above, with  $N = 31 \times 10^6$  atoms in one (two) wells, we get a temperature of  $1.7$  ( $1.3$ )  $\mu\text{K}$ . The true prediction lies somewhere in between, since there are two minima whose relative population depends on the laser alignment and profile, which we can control only with limited precision. A systematic underestimate of the atom numbers may be responsible for the higher temperature measured. The agreement between theory and prediction is reasonable given the uncertainties in the exact shape of the potential due to beam alignment as well as the effects of anharmonicity.

Below the transition, we studied the anisotropic expansion of the condensate. Assuming harmonic confinement, in the Thomas-Fermi limit the chemical potential  $\mu$  is related to the expanded cloud sizes through the relation  $\mu = M/(4t^2)(W_x^2 + W_y^2 + W_z^2)$  where  $W_i$  is the Thomas-Fermi radius along the  $i$ th direction obtained from a parabolic fit to the time-of-flight image. For our geometry, roughly 65%, 25%, and 10% of the energy is released in the  $y$ ,  $z$ , and  $x$  directions, respectively. We estimate  $\mu/k_B = 600 \text{ nK}$  from the measured cloud sizes. The Thomas-Fermi prediction is  $\mu = (15^{2/5}/2)(Na_s/\bar{a})^{2/5}\hbar\bar{\omega}$  where  $N$  is the number of condensed atoms,  $a_s = 2.75 \text{ nm}$  is the scattering length, and  $\bar{a} = \sqrt{\hbar/(M\bar{\omega})}$  is the harmonic oscillator length [14]. Estimating the atom number to be  $\approx 20 \times 10^6$  atoms in one (two) wells, we compute  $\mu/k_B = 530$

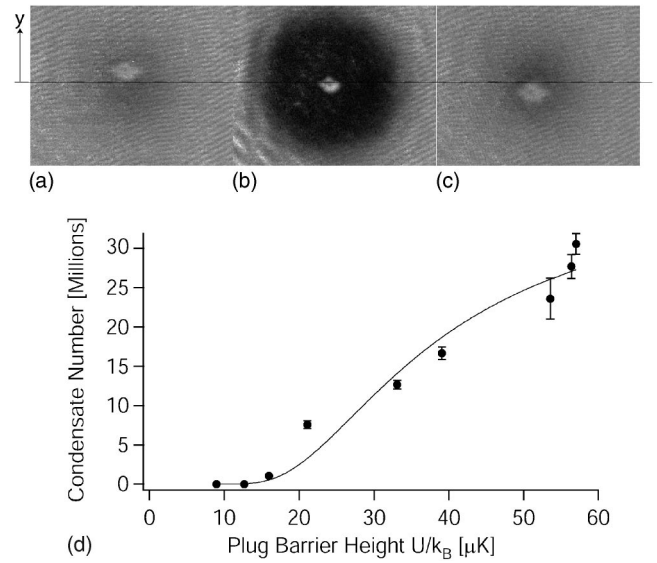


FIG. 3. Plugging the hole. Catastrophic loss results if the “plug” is not carefully aligned. In (b) it is aligned precisely with the magnetic field zero (indicated by a dashed line), resulting in a large number of atoms near the end of the rf evaporation stage, while in (a) and (c) it is misaligned along the  $y$  direction by  $+90$  and  $-65 \mu\text{m}$ , respectively, resulting in very few atoms. The field of view in each image is  $1 \times 1 \text{ mm}^2$ . The plug laser power also dramatically affects the number of condensate atoms achieved, as shown in (d) (closed circles), although large condensates were obtained even when the plug is not completely capable of repelling atoms loaded from the MOT, whose initial temperature was  $T_i = 190 \mu\text{K}$ . Each point is the average of between two and four separate runs of the experiment, and the error bars are statistical. The solid line is a fit of the data to a model described in the text.

(400) nK. Both release energy and transition temperature are slightly higher than the predictions, as would be expected for an underestimate of the atom number.

We explored the crucial role played by the plug during evaporation. Figure 3 demonstrates how strong Majorana losses are—when the plug beam was misaligned from the magnetic field center by more than  $50 \mu\text{m}$  along any direction [Figs. 3(a) and 3(c)], tremendous losses ensued and very few atoms remained near the end of the evaporation ramp. However, when it was correctly aligned, as in Fig. 3(b), we obtained a huge increase in probe absorption, an unmistakable signature that the hole had been successfully plugged and that we could produce a BEC.

While the plug beam is clearly necessary, a natural question is how high the potential barrier must be to prevent Majorana loss. We varied the laser power and therefore the barrier height  $U$ , observing the final atom number in the condensate, with the results plotted in Fig. 3(d). Two features are distinctly visible. For one, there is a threshold barrier  $U = U_c$  for observing a condensate corresponding to about  $15 \mu\text{K}$  (we have observed that  $U_c$  depends on the loading conditions). Second, there is a roughly linear increase in the number of atoms with no clear evidence of saturation as  $U$  is raised up to  $60 \mu\text{K}$ , corresponding to the maximum power available from the laser. We estimate that the atom number should saturate when  $U > U_{\text{max}} = \frac{3}{2}k_B T_i \approx 300 \mu\text{K}$ , the aver-

age energy of atoms passing near the hole at the beginning of evaporation. Indeed, we estimate that  $U=60 \mu\text{K} < U_{\max}$  at our maximum power from the measured laser power and beam size [15]. Remarkably, in spite of some Majorana loss, BECs of up to  $30 \times 10^6$  atoms could still be created, close to the state of the art achieved in IP traps. By using a tighter focus of  $15\text{--}20 \mu\text{m}$ , it may be possible, therefore, to use a plug laser whose power is 1 W or lower, rather than the 5-W version currently in use.

We can explain our observations qualitatively by noting that Majorana loss is most significant at low temperatures, and should disappear for  $U > U_{\max}$ . In this limit, we expect the largest condensate atom number  $N_c = N_c^{\max}$ . If  $U < U_{\max}$  there will be loss for a period  $T > T_{\min}$  and no loss for  $T < T_{\min} = 2U/(3k_B)$ , resulting in a condensate with  $N_c < N_c^{\max}$ . If  $U$  is less than some critical value  $U_c$ , the losses are sufficiently high so that evaporative cooling cannot be sustained and no BEC is formed, as observed for our data at  $U \approx k_B \times 15 \mu\text{K}$ . The key point is that a BEC can still be produced in the intermediate regime  $U_c < U < U_{\max}$ , i.e., in the presence of finite (but not overwhelming) losses.

To quantify this further, we introduce a simple model that describes the essential physics in this regime. We can compute an analytical expression for the ratio  $N_c/N_c^{\max}$ . To this end, we include Majorana loss in Eq. (9) of Ref. [16] and integrate with respect to time, writing all quantities in terms of temperature. This results in the following expression for the phase space density  $D$ :

$$\ln \frac{D}{D_i} = \tilde{\alpha} \ln \frac{T}{T_i} + \frac{\tau_{ev}}{\alpha} \int_{T_i}^T \Gamma_M \frac{dT'}{T'} \quad (1)$$

where  $T_i$  and  $D_i$  are, respectively, the temperature and phase space density at the start of evaporation,  $\alpha$  expresses logarithmically the change in temperature per atom evaporated,  $\tilde{\alpha} = [1 - \alpha(\delta + 3/2)]/\alpha$ , where  $\delta = 3$  for a three-dimensional linear potential, and  $\tau_{ev}$  is the time constant for atom number decay, assumed, for simplicity, to be independent of temperature and any (small) losses. Note that  $\tilde{\alpha} < 0$ .  $\Gamma_M$  is the Majorana loss rate, which we calculate as follows. Ref. [9] estimates the rate at which atoms pass through the Majorana ‘‘hole’’ in a linear trap to be  $\Gamma_M = C/T^2$ , where  $C$  is a constant that depends on  $\mu B'$ . In the presence of the plug, the atoms must climb an energy barrier  $U$  to get to the hole, which modifies the atomic velocity from  $v = \sqrt{2E/M}$  to  $\sqrt{2(E-U)/M}$ , where  $E = \frac{3}{2}k_B T$  is the energy. Since the loss rate is proportional to  $v^2$  [9], this gives a corrected estimate of  $\Gamma_M = (C/T^2)(1 - 2U/3k_B T)$ . Physically, by climbing up the ‘‘plug’’ potential, the atom slows down, and Majorana transitions are suppressed since it perceives the magnetic field change to be more adiabatic.

Equation (1) applies during the loss period  $T > T_{\min}$ , whereas for  $T < T_{\min}$  we have evaporative cooling without loss:

$$\ln \frac{D}{D_{\min}} = \tilde{\alpha} \ln \frac{T}{T_{\min}} \quad (2)$$

where  $D_{\min}$  is given by Eq. (1) evaluated at  $T = T_{\min}$ . Condensation occurs when  $D = D_c = 2.612$ , at a temperature of  $T_c$ . To

account for this, we assume that evaporation proceeds to essentially zero temperature, where the final condensate number  $N_c$  is a fixed fraction of the number of thermal atoms at  $T = T_c$  (typically, about 1/3), and therefore  $N_c \propto T_c^3$  for a harmonic potential. It is then straightforward to combine Eqs. (1) and (2), eliminating  $D_c$  and  $D_i$  to write

$$\frac{\tilde{\alpha}}{3} \ln \frac{T_c}{T_c^{\max}} = - \frac{\tau_{ev}}{\alpha} \int_{T_i}^{T_{\min}} \Gamma_M \frac{dT}{T}. \quad (3)$$

We then put  $T_{\min} = 2U/(3k_B)$  and perform the integration using the above expression for  $\Gamma_M$  to obtain a final answer of

$$N_c = N_c^{\max} \exp \left( - \frac{3}{R\tilde{\alpha}} \left[ 1 - \left[ \frac{3k_B T_i}{2U} \right]^2 - \frac{4U}{9k_B T_i} \times \left( 1 - \left[ \frac{3k_B T_i}{2U} \right]^3 \right) \right] \right) \quad (4)$$

where  $N_c^{\max}$  occurs at  $U = U_{\max} = 3/2k_B T_i$  and  $R = (2\alpha/\tau_{ev})(T_i^2/C)$  is essentially the ratio of the rates of evaporative cooling and Majorana loss. Equation (4) is plotted as a solid line in Fig. 3 using  $T_i = 190 \mu\text{K}$ , with a two-parameter fit to the data yielding  $N_c^{\max} = 3.7 \times 10^7$  atoms and  $|R \times \tilde{\alpha}| = 75$ . Both parameters are quite reasonable for our conditions.  $N_c^{\max}$  is about 25% larger than our maximum observed atom number. We can compare the fit value for  $|R \times \tilde{\alpha}|$  with an order of magnitude estimate based on our experimental parameters. With a factor of  $\sim 15$  (20) reduction in atom number (temperature) over the first 27s of evaporation we deduce  $\tau_{ev} \approx 10$  s and  $\alpha \approx 1$ . An order of magnitude estimate assuming no plug is present gives  $C \sim \hbar/M(2\mu B'/(3k_B))^2 = 1400 (\mu\text{K})^2 \text{s}^{-1}$  [9], whereas we take an upper bound on  $C$  of  $400 \mu\text{K}^2 \text{s}^{-1}$  from the 90-s lifetime for atoms at the highest temperatures. The end result is  $|R \times \tilde{\alpha}| \approx 60$ , fortuitously close to the fit value.

Over the range of  $15 < U < 60 \mu\text{K}$ , the model predicts a smooth variation in atom number rather than a sharp threshold, in agreement with our data. The latter does not clearly show the saturation present in the model, however. A more complete model would account for the time variation of  $\tau_{ev}$  (i.e., ‘‘runaway’’ evaporation), the effect of Majorana loss on the atoms energy distribution (possible heating or cooling), and the dynamics of condensation (going beyond the treatments of [16,17]). However, our simple treatment appears sufficient to grasp the essential physics, namely, that evaporation in the presence of small losses can still successfully produce large condensates.

Finally, we demonstrate that the OPT can be used as a ‘‘cooling stage’’ to achieve quantum degeneracy, followed by transfer of atoms (in a procedure similar to [8]) into a purely optical trap formed by a single, focused infrared laser beam. Here the atoms are localized near the intensity *maximum*, where the potential energy surface is well defined. Our trap was formed by the output of a 1064-nm fiber laser which passed through an AOM and a single-mode optical fiber before being focused onto the atoms with a beam waist of

roughly  $25 \mu\text{m}$ . In spite of a significant mode mismatch between the OPT and the purely optical trap, we achieved a transfer of up to  $9 \times 10^6$  atoms, or 50 % of the condensate.

In conclusion, we have demonstrated a state-of-the-art, large-volume magnetic trap for Bose-Einstein condensation. Future designs incorporating a quartz cell vacuum chamber would benefit the most from the enhanced optical access of the OPT. For example, one would achieve unrestricted access

along two axes, rather than just one, as is typical of Ioffe-Pritchard traps such as the cloverleaf design [11].

We thank W. Ketterle and T. A. B. Kennedy for useful discussions, A. Traverso, G. Belenchia, P. Gabolde, and B. Kaiser for experimental assistance, and M. S. Chapman for a critical reading of the manuscript. This work was supported by the DOE and GT startup funds.

- 
- [1] See E. A. Cornell *et al.* in Bose-Einstein Condensation in Atomic Gases, Proceedings of the International School of Physics “Enrico Fermi,” Course CXL, edited by M. Inguscio, S. Stringari, and C. E. Wieman, Amsterdam, 1999; W. Ketterle *et al.*, *ibid.*
- [2] M. D. Barrett, J. A. Sauer, and M. S. Chapman, Phys. Rev. Lett. **87**, 010404 (2001).
- [3] S. R. Granade, M. E. Gehm, K. M. O’Hara, and J. E. Thomas, Phys. Rev. Lett. **88**, 120405 (2002).
- [4] T. Weber, J. Herbig, M. Mark, H. C. Nagerl, and R. Grimm, Science **299**, 232 (2003).
- [5] K. B. Davis, M.-O. Mewes, M. R. Andrews, N. J. van Druten, D. S. Durfee, D. M. Kurn, and W. Ketterle, Phys. Rev. Lett. **75**, 3969 (1995).
- [6] J. R. Abo-Shaeer, C. Raman, J. M. Vogels, and W. Ketterle, Science **292**, 476 (2001).
- [7] A. Görlitz, T. L. Gustavson, A. E. Leanhardt, R. Löw, A. P. Chikkatur, S. Gupta, S. Inouye, D. E. Pritchard, and W. Ketterle, Phys. Rev. Lett. **90**, 090401 (2003).
- [8] D. M. Stamper-Kurn, M. R. Andrews, A. P. Chikkatur, S. Inouye, H.-J. Miesner, J. Stenger, and W. Ketterle, Phys. Rev. Lett. **80**, 2027 (1998).
- [9] W. Petrich, M. H. Anderson, J. R. Ensher, and E. A. Cornell, Phys. Rev. Lett. **74**, 3352 (1995).
- [10] M. H. Anderson, J. R. Ensher, M. R. Matthews, C. E. Wieman, and E. A. Cornell, Science **269**, 198 (1995).
- [11] M. O. Mewes, M. R. Andrews, N. J. van Druten, D. M. Kurn, D. S. Durfee, and W. Ketterle, Phys. Rev. Lett. **77**, 416 (1996).
- [12] W. Ketterle, K. B. Davis, M. A. Joffe, A. Martin, and D. E. Pritchard, Phys. Rev. Lett. **70**, 2253 (1993).
- [13] F. Dalfovo, S. Giorgini, L. P. Pitaevskii, and S. Stringari, Rev. Mod. Phys. **71**, 463 (1999).
- [14] C. J. Pethick and H. Smith, *Bose-Einstein Condensation in Dilute Gases* (Cambridge University Press, Cambridge, U.K., 2002).
- [15] This estimate includes a 25% increase in beam size as the power was raised to its full value due to thermal effects in the optics. The beam alignment with the field zero remained unchanged to within the experimental resolution, about  $5 \mu\text{m}$ .
- [16] W. Ketterle and N. J. van Druten, Adv. At., Mol., Opt. Phys. **37**, 181 (1996).
- [17] O. J. Luiten, M. W. Reynolds, and J. T.M. Walraven, Phys. Rev. A **53**, 381 (1996).